Monte Carlo simulation study of mesophase formation in dipolar spherocylinders

D. Levesque, J. J. Weis, and G. J. Zarragoicoechea*
Laboratoire de Physique Théorique et Hautes Energies, Bâtiment 211, Université de Paris-Sud, 91405 Orsay CEDEX, France
(Received 30 July 1992)

The influence of dipolar forces on the structural and thermodynamic properties of hard spherocylinders is investigated in the isotropic and smectic phases using Monte Carlo simulations. Irrespective of the characteristics of the dipole moment, location (from center to the end of the molecule), strength (μ^* varying from 0 to $\sqrt{6}$), and direction (from parallel to perpendicular to the molecular axis), the stable smectic-A phase is found to have a monolayer structure. In the case of a longitudinal dipole moment the layers are unpolarized; for transverse dipole moments the simulation results give some indication for a net polarization of the system parallel to the smectic planes, although this result should be taken with care because of the slow relaxation of the system towards equilibrium.

PACS number(s): 61.30.−v, 61.20.Ja, 61.25.Em, 64.70.Md

I. INTRODUCTION

Thermotropic low-molecular-weight liquid crystals can be broadly divided into two classes according to their overall shape—rodlike and disklike [1]. Extensive computer-simulation studies [2–9] over the past decade have shown that simple hard-core models having rodlike or disklike shape show mesophase behavior similar to that observed in real liquid crystals. The purpose of the present paper is to use Monte Carlo simulations to show how for rod-shaped molecules this behavior is affected by dipolar interactions present in a large variety of mesogenic molecules. In a separate paper we investigate the effect of dipolar interactions in disklike molecules [10].

Liquid-crystal molecules with strongly polar head groups exhibit a much richer phase diagram than the more conventional liquid crystals [11]. The differences are manifested most strikingly in the formation of a number of smectic-A (Sm-A) phases [11] and the occurrence of Sm-A–Sm-A transitions [12], as well as reentrant phenomena [13] in which the less ordered phase (e.g., nematic) reappears upon lowering the temperature from the more ordered phase (e.g., smectic). A phenomenological understanding of the phase behavior of strongly polar liquid crystals has been provided by Prost [14] using a mean-field theory in which the conventional order parameter describing the density wave along the direction of alignment of the molecules (director) is coupled to a second-order parameter describing the dipolar ordering of the molecules along this direction. The phase behavior results from a competition between these two order parameters.

The commonly observed smectic-A phases are the monolayer (Sm-A_1), bilayer (Sm-A_2) and partial bilayer (Sm-A_d) phases [11]. In the monolayer Sm-A_1 phase, the smectic layer spacing δ is of the order of the molecular length l and the dipolar heads are oriented randomly within each layer. The Sm-A_2 phase has bilayer structure with period comparable to two molecular lengths. Each layer (within the bilayer) has preferential dipolar ordering alternating in direction from one layer to the other. The Sm-A_d phase is the most frequently observed in thermotropic amphiphilic liquid crystals [11]. In this phase the layer spacing is $l < \delta < 2l$ (a typical value is $\delta \sim 1.4l$), and the structure is believed to result from the partial overlap of the molecular cores due to antiparallel dipolar interactions [11]. Although the unique role of dipolar interactions in producing these phases is now well established, a quantitative correlation between phase behavior and molecular parameters, such as structure and polarizability of the core region and characteristics of the dipole moments and of the hydrocarbon chains, has not yet been fully established. Despite considerable experimental effort devoted to this problem, the subtle interplay of the various above-mentioned factors has so far precluded a quantitative assessment of the role played by each of these factors in mesophase formation and stabilization.

The present paper is an attempt to determine by Monte Carlo simulations the contribution of the dipole interaction to mesophase formation in a simple system of axially symmetric hard-core molecules (spherocylinders) with point dipole moment located at the center of the molecule, at one of the ends (head), or at some intermediate distance between center and head. In addition, three directions of the dipole were considered, making angles 0°, 60°, and 90° with the molecular long axis. The model will be described in more detail in Sec. II, which also contains the technical details of the computations. Results for the orientational order in the isotropic and smectic phases will be given in Sec. III and contrasted with those obtained for nonpolar molecules. The conclusions are given in Sec. IV.

II. MODEL AND METHOD

The system consists of hard spherocylinders of length-to-breadth ratio $L/D+1=6$ (L, length of the cylindrical part; D, diameter) with the dipole moment located at a distance $d=0$, 1.5, or 2.5 (in units of D) from the center of the spherocylinder (in the latter case the dipole moment is located at the center of one of the hemispherical

caps). The angle between the direction of the dipole moment and the molecular symmetry axis, oriented from the center of the molecule to the dipole moment, is $\theta=0°$ (longitudinal dipole moment), 60°, and 90° (transverse). The magnitude of the dipole moment (in reduced units) covers the range from $\mu^*=(\mu^2/D^3kT)^{1/2}=0$ to $\sqrt{6}$ encompassing the high values encountered in liquid crystals with strongly polar cyano or nitro terminal groups. In the isotropic phase, the Monte Carlo calculations were performed in the canonical (NVT) ensemble using a cubic simulation cell with periodic boundary conditions. In the smectic phase calculations were carried out in the isothermal-isobaric ensemble (NpT) and an orthorhombic simulation cell with side lengths L_x, L_y and L_z (with periodic boundary conditions) was chosen in order to accommodate easily an appropriate number of smectic layers.

The long-range dipolar interactions superimposed on the hard-core interactions were taken into account by the Ewald summation method as described in Refs. [15] and [16]. Specifically, the dipole-dipole interaction is calculated from

$$U=-\tfrac{1}{2}\sum_{\substack{i,j\\(i\neq j)}}(\boldsymbol{\mu}_i\cdot\nabla)(\boldsymbol{\mu}_j\cdot\nabla)\frac{\operatorname{erfc}(\alpha|\mathbf{r}_{ij}|)}{|\mathbf{r}_{ij}|}+\frac{1}{2\pi V}\sum_{\substack{\mathbf{k}\\(\mathbf{k}\neq 0)}}\frac{4\pi}{\mathbf{k}^2}e^{-\mathbf{k}^2/4\alpha^2}|F(\mathbf{k})|^2\ , \tag{1}$$

where

$$F(\mathbf{k})=\sum_i(\mathbf{u}_i\cdot\mathbf{k})e^{i\mathbf{k}\cdot\mathbf{r}_i}\ . \tag{2}$$

In Eqs. (1) and (2), $\mathbf{r}_i$ denotes the position of dipole moment $\boldsymbol{\mu}_i$ in molecule i, $|\mathbf{r}_{ij}|=|\mathbf{r}_j-\mathbf{r}_i|$, and $V=L_xL_yL_z$ is the volume of the basic simulation cell. The reciprocal space vectors $\mathbf{k}$ are of the form

$$\mathbf{k}=\left[\frac{2\pi}{L_x}n_x,\frac{2\pi}{L_y}n_y,\frac{2\pi}{L_z}n_z\right],$$

where n_x, n_y, and n_z are positive or negative integers. The parameter α which governs the convergence of the real-space and reciprocal-space contributions to the energy was taken equal to $\alpha L_{\min}\sim 5.6$ [$L_{\min}=\min(L_x,L_y,L_z)$]. With this value of α, the real-space contribution can be restricted to the first term shown in (1). It was evaluated by summing over *all* pairs of particles inside the simulation cell. The reciprocal-space term [second term in (1)] included all $\mathbf{k}$ vectors such that

$$|\mathbf{n}|^2=n_x^2+n_y^2+n_z^2\leq 25\ ,$$

and this for all box shapes considered.

The orientational order of the system was characterized by the order parameter S defined as the average value of the largest eigenvalue of the second-rank tensor

$$\overleftrightarrow{Q}=\frac{1}{2N}\sum_{i=1}^{N}(3\hat{\mathbf{u}}_i\hat{\mathbf{u}}_i-\overleftrightarrow{I})\ , \tag{3}$$

where $\hat{\mathbf{u}}_i$ is a unit vector along the symmetry axis of the molecule and N denotes the number of molecules in the system.

III. RESULTS

A. Isotropic phase

The isotropic phase of hard spherocylinders of elongation $L/D=5$ has been shown to extend, in the absence of dipolar interactions, up to a density $\rho D^3=0.089$ at which the onset of a nematic phase occurs [4]. In order to investigate the effect of a dipolar interaction on thermodynamic and structural properties, we have carried out Monte Carlo simulations (NVT ensemble) on a system of 448 spherocylinders in a cubic box with either zero dipole moment or strong longitudinal or transverse dipole moment ($\mu^*=2.449$) located at the center of the molecule. Energy and pressure values obtained at density $\rho^*=\rho D^3=0.07$ are summarized in Table I. The hard-core part of the pressure was calculated along the lines described in Ref. [17] by exhibiting an analytical function F having the property that $F<1$ if two molecules overlap and $F>1$ if they do not. For the case of spherocylinders, the function F is the square of the shortest distance between the two line segments joining the centers of the hemispherical caps. For the case of a central dipole moment, the contribution p_d to the pressure due to the dipolar interactions is related to the energy through the equation $p_d/\rho kT=U/NkT$. For $\mu^*=0$ we find a pressure in complete agreement with the value given by Frenkel for a 576-particle system [4]. The center-of-mass distribution function $g^{000}(r)$ and the dipole-dipole correlation function $h^{110}(r)$ defined by

$$h^{110}(r)=\frac{3}{N}\sum_{\substack{i,j\\(i\neq j)}}\langle\hat{\mathbf{s}}_i\cdot\hat{\mathbf{s}}_j\delta(\mathbf{r}_i-\mathbf{r}_j-\mathbf{r})\rangle\ , \tag{4}$$

where $\hat{\mathbf{s}}_i$ is a unit vector along the direction of the dipole moment of molecule i, are shown in Figs. 1 and 2, respectively. From these figures it is apparent that for nonpolar molecules or molecules with longitudinal dipole moment, positional and angular correlations are limited to nearest-neighbor distances. The correlations are, however, much stronger for the polar molecules with preferential antiparallel orientation of neighboring dipole moments, similar to what has been observed previously for dipolar ellipsoids [18,19].

In the case of a transverse dipole moment, the positional and orientational orders are strongly correlated over three nearest-neighbor distances with preferential lateral contact of the cylinders and parallel orientation of the dipole moments. Notice the well-defined peaks in g^{000} and h^{110} at $r/D=1,2,3,4$ in strong contrast with the case $\mu^*=0$. Such an arrangement is compatible with the low dipole-dipole energy (cf. Table I) found in this case. In all cases the order parameter was nearly zero, indicating that the systems were orientationally isotropic. This is confirmed by inspection of the h^{220} projection which decays to zero at $r/D\sim 4$ (cf. Fig. 3; for a definition of h^{220}, see Ref. [18]). It is quite interesting to remark that

TABLE I. Thermodynamic properties, pressure p^*, density ρ^*, and internal energy U/NkT of a system of dipolar spherocylinders of length $L/D=5$ in the isotropic and smectic phases as a function of dipole-moment strength μ^*, location d (in units of cylinder diameter D) from the center of the molecule, and direction θ (in degrees) with respect to the molecular symmetry axis. The reduced quantities are defined as $\mu^*=(\mu^2/D^3kT)^{1/2}$, $p^*=pD^3/kT$, and $\rho^*=\rho D^3$, where T is the temperature, k the Boltzmann constant, and N the number of molecules. n denotes the number of trial moves per molecule.

μ^*	d	θ	Ensemble	n	p^*	ρ^*	U/NkT
			Isotropic phase				
0			NVT	20 000	0.58	0.07	0
2.449	0	0	NVT	20 000	0.48	0.07	−1.39
2.449	0	90	NVT	30 000	0.36	0.97	−9.7
			Smectic phase				
1.414	2.5	0	NpT	80 000	3.8	0.127	−0.32
2.0	2.5	0	NpT	80 000	3.8	0.128	−1.04
2.449	2.5	0	NpT	80 000	3.8	0.126	−2.04
2.0	2.5	60	NpT	80 000	3.8	0.130	−4.66
2.449	2.5	60	NpT	40 000	3.8	0.133	−8.63
2.0	2.5	90	NpT	60 000	3.8	0.133	−6.32
2.449	2.5	90	NpT	40 000	3.8	0.133	−11.02
2.449	1.5	0	NpT	40 000	3.8	0.128	−0.59
2.449	1.5	90	NpT	40 000	3.8	0.130	−7.44
2.0	0	60	NpT	40 000	3.8	0.137	−4.09
2.449	0	60	NpT	40 000	3.8	0.136	−7.74
0			NVT	40 000	2.85	0.130	0
0			NpT	80 000	3.8	0.135	0

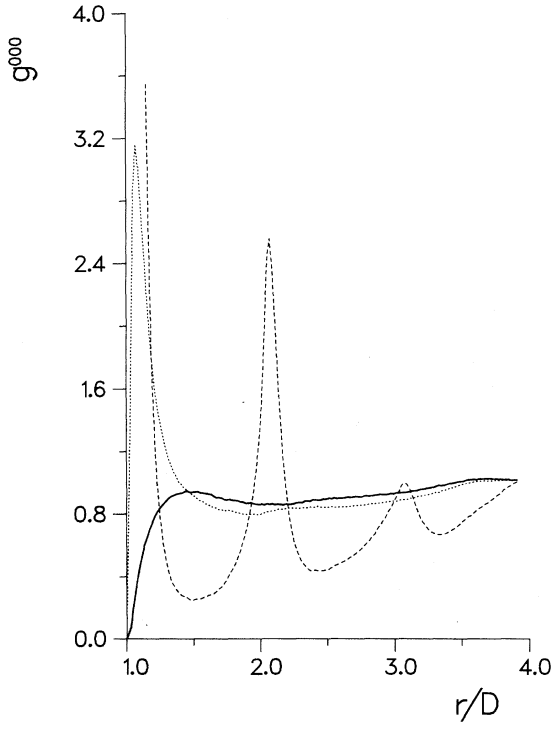

FIG. 1. Center-of-mass pair distribution function $g^{000}(r)$ for dipolar spherocylinders of length $L/D=5$ and density $\rho^*=0.07$ (isotropic phase). Dotted line, longitudinal central dipole moment $\mu^*=2.449$; dashed line, transverse central dipole moment $\mu^*=2.449$; the peak height near $r/D=1$ is ~20; solid line, nonpolar spherocylinders $\mu^*=0$.

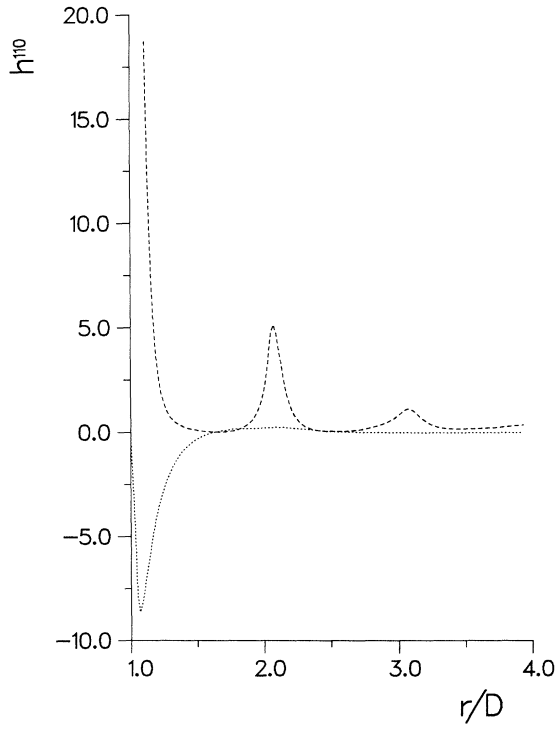

FIG. 2. Dipole-dipole correlation function $h^{110}(r)$ [Eq. (4)] for dipolar spherocylinders of length $L/D=5$ and density $\rho^*=0.07$ (isotropic phase). Dotted line, longitudinal central dipole moment $\mu^*=2.449$; dashed line, transverse central dipole moment $\mu^*=2.449$; the peak height near $r/D=1$ is ~50 in this case.

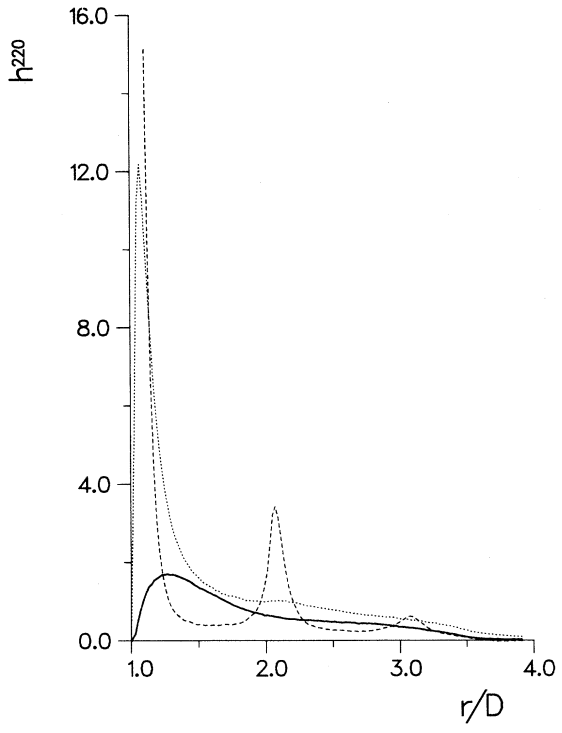

FIG. 3. Orientational correlation function $h^{220}(r)$ for dipolar spherocylinders of length $L/D=5$ and density $\rho^*=0.07$ (isotropic phase). Dotted line, longitudinal central dipole moment $\mu^*=2.449$; dashed line, transverse central dipole moment $\mu^*=2.449$; the peak height near $r/D=1$ is ~ 40; solid line, nonpolar spherocylinders $\mu^*=0$.

strong parallel association of the dipole moments has been observed recently in dipolar cyano-substituted molecules with transverse dipole moment dissolved in a nonpolar nematic liquid-crystal solvent [20].

B. Smectic phase

In the smectic phase the differences in polymorphic behavior between polar and nonpolar systems are expected to be largest, and therefore this phase has been studied in greatest detail. The Monte Carlo simulations were performed with 384 molecules in the isothermal-isobaric ensemble at fixed pressure $p^*=pD^3/kT=3.8$. An initial configuration of the spherocylinder system was generated from a close-packed structure with hexagonal symmetry within layers parallel to the xy plane and $ACAC\ldots$ stacking sequence of the planes along the z direction. The number of layers in the x, y, and z directions was $N_x=8$, $N_y=8$, and $N_z=6$. Initially all dipole moments were aligned in the same direction parallel to the z-axis. The system was then expanded uniformly in all directions and equilibrated at pressure $p^*=3.8$ with a longitudinal dipole moment $\mu^*=\sqrt{2}$ located at a distance $d=2.5$ from the molecular center. A stable smectic phase was found having density $\rho^*=0.127$. In subsequent runs in which location, strength, and direction of the dipole moments were varied, the initial configuration was taken to be that of a previous equilibrated run.

In the sampling of configuration space, allowance was made, besides translation and rotation, for flips of the molecular long axis in order to generate polarized as well as unpolarized smectic layer configurations. Volume changes were made by scaling the box dimensions in the x, y, and z directions independently.

The thermodynamic properties of the different runs are summarized in Table I. The densities were generally slow to converge (more than 50 000 moves per particle are needed), and the statistical error is estimated to be ~ 0.004. In the present calculations, in order to accommodate a reasonable number of smectic layers (six layers), an orthorhombic box shape with dimension much larger in the z direction ($L_z\sim 38.8D$) than in the x or y directions ($L_x\sim 9.5D$, $L_y\sim 8.4D$) was used. The influence of the box dimensions on the pressure appears to be nonnegligible. With an orthorhombic box the density at $\mu^*=0$ and $p^*=2.85$ is found to be $\rho^*=0.130$, whereas for a nearly cubic simulation cell ($L_x\simeq L_y\simeq L_z\sim 16D$), this density value is obtained for a pressure which is about 20% lower ($p^*\sim 2.2$) [4].

From Table I it is apparent that for fixed pressure the density depends only little (within statistical error) on dipole-moment strength and direction. However, it would seem that the density decreases slightly when the location of the dipole moment is moved from the center to one of the ends of the spherocylinder.

Smectic ordering along the direction perpendicular to the smectic planes (here the z axis) has been analyzed by the following correlation functions:

$$f(i\Delta z)=\frac{\left\langle \sum_{j=0}^{m} n(j\Delta z)n[(i+j)\Delta z]\right\rangle}{m\rho^{*2}S_{xy}^2\Delta z^2} \quad (i\neq 0)\,, \tag{5}$$

where $n(z)$ is the number of particles having the z coordinate of their center of mass or dipole location in the interval $(z,z+\Delta z)$, $m=L_z/\Delta z$, $S_{xy}=L_xL_y$, ρ^* is the average density of the system, and $\Delta z=0.02D$. These functions have been calculated for various locations, strengths, and directions of the dipole moments. Most of the results pertain to the case where the dipole is located at the head of the spherocylinder ($d=2.5$) for this would be the case encountered in most strongly polar mesogens.

1. $d=2.5$

The influence of the magnitude of a longitudinal dipole moment, when $d=2.5$, on the density waves of the center of mass and the polar head has already been discussed in Ref. [21]. Here we present additional results obtained when the direction of the dipole moment is varied (Figs. 4 and 5). In all cases considered, the density waves of both the center of mass and the polar head have the *same* period. If one defines the smectic layer spacing δ as the distance between two peaks in the density wave of the center of mass, one finds $\delta\sim 6.3$, a value slightly larger than one molecular length. While the period of the density wave is independent of dipole-moment characteristics, the amplitude and width, on the contrary, de-

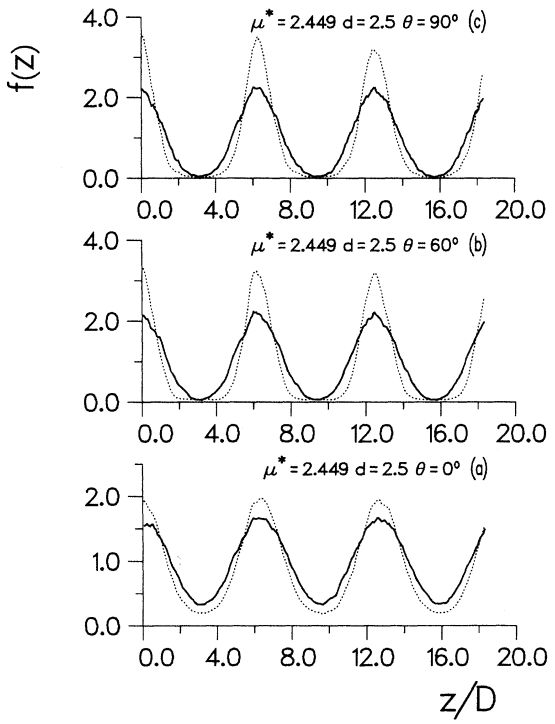

FIG. 4. Density modulation [Eq. (5)] of the smectic-A phase of dipolar spherocylinders with $\mu^*=2.449$, $d=2.5$ as a function of dipole-moment direction. The pressure is $p^*=3.8$. Solid line, center-of-mass density; dotted line, density of dipole-moment positions. (a) $\theta=0°$; (b) $\theta=60°$; (c) $\theta=90°$.

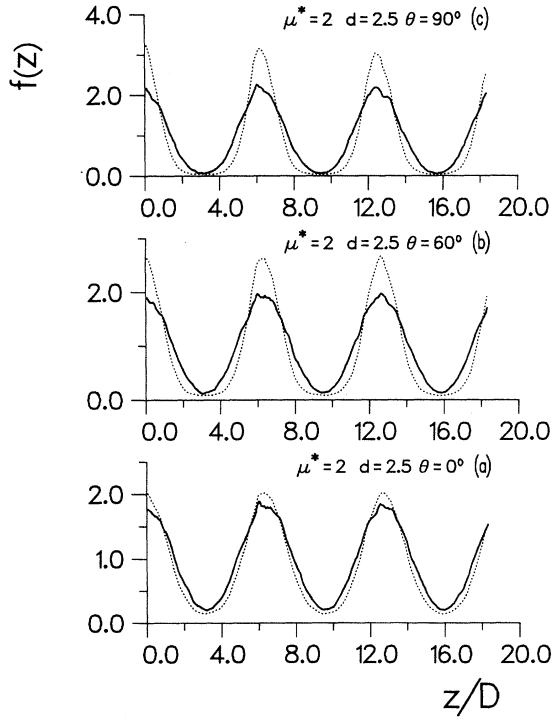

FIG. 5. Density modulation [Eq. (5)] of the smectic-A phase of dipolar spherocylinders with $\mu^*=2.0$, $d=2.5$ as a function of dipole-moment direction. The pressure is $p^*=3.8$. Solid line, center-of-mass density; dotted line, density of dipole-moment positions. (a) $\theta=0°$; (b) $\theta=60°$; (c) $\theta=90°$.

pend more appreciably on them. In Ref. [21] we have shown that for a longitudinal dipole moment, the polar head positions become increasingly more localized with increasing dipole-moment strength, while those of the center of mass get more diffuse. Figure 4 shows, for $\mu^*=2.449$, that the localization of the polar head is even stronger when the angle of dipole-moment direction with respect to the molecular long axis increases from 0 (longitudinal) to 90 (transverse), while that of the center-of-mass positions increases only sightly. Similar observations are made for the smaller dipole moment $\mu^*=2$ (cf. Fig. 5). Snapshots of the system, representing projections of the system on the xz plane of the simulation cell (recall that the smectic layer normal is along the z axis), demonstrate these findings in an even more illustrative way. Figures 6, 7, and 9 show projections of all the molecules on the xz plane, whereas Figs. 8 and 10 show only molecules within a slice of width $\Delta y \simeq 2D$ in the y direction (note that in Figs. 6, 7, and 9, for the sake of clarity, the horizontal scale has been expanded with respect to the vertical scale, but that the relative dimensions of the xz plane of the simulation cell have been preserved in Figs. 8 and 10).

Inspection of the snapshots allows several more conclusions concerning the molecular arrangement within the smectic layers. In the case of a longitudinal dipole moment, it is seen that within each layer there is approximately an equal number of molecules with dipole moments pointing "up" and "down," so that the layers have no net polarization (cf. Figs. 7 and 8). This result has

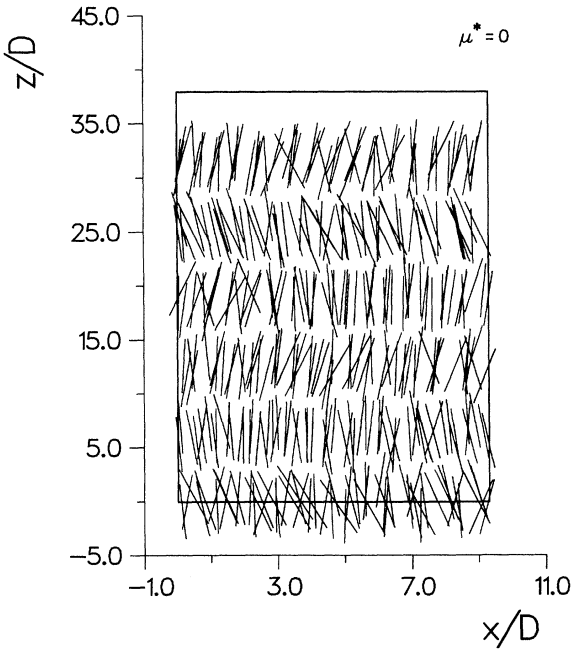

FIG. 6. Snapshot of a configuration of 384 spherocylinders without dipole moment in the smectic-A phase (projection on the xz plane of the periodic box; the molecules are represented by thin lines of length $5D$). The pressure is $p^*=3.8$. Note that the scale in the x direction is expanded with respect to that in the z direction.

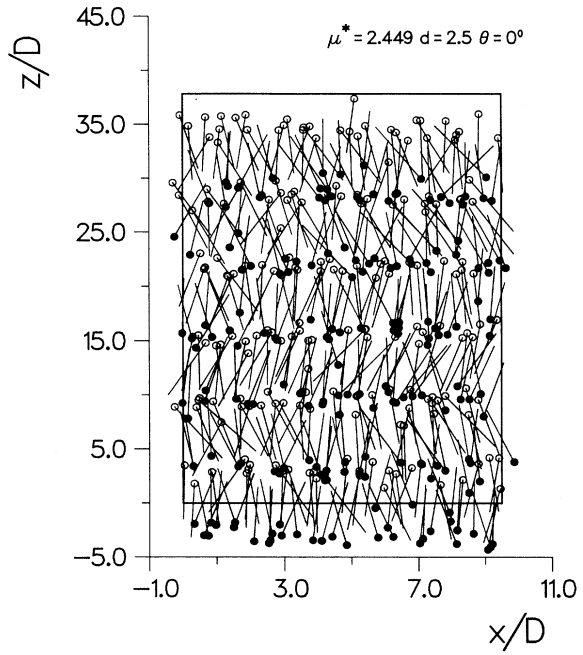

FIG. 7. Snapshot of a configuration of 384 spherocylinders with longitudinal dipole moment $\mu^*=2.449$ located at distance $d=2.5$ from the center of the molecule in the smectic-A phase ($p^*=3.8$) (projection on the xz plane of the periodic box; the molecules are represented by thin lines of length $5D$). Open circles, dipole moments pointing in the positive z direction; solid circles, dipoles pointing in the negative z direction. Note that the scale in the x direction is expanded with respect to that in the z direction.

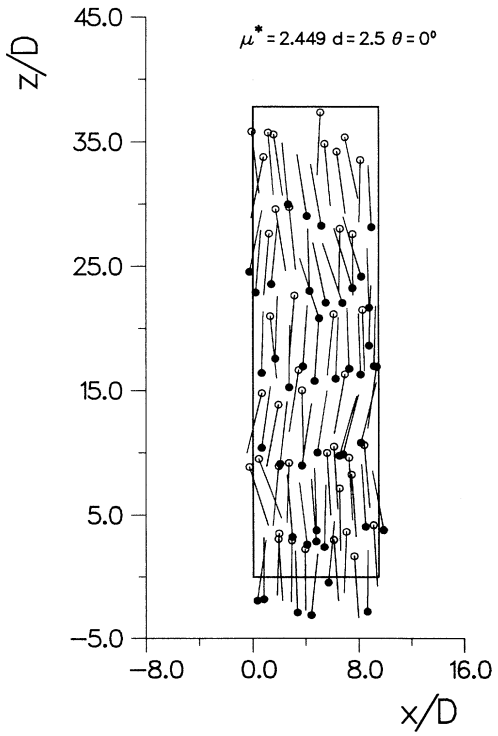

FIG. 8. Same as Fig. 7, but for molecules in a slice of width $\Delta y \simeq 2D$ in the y direction. The scales in the x and z directions are identical.

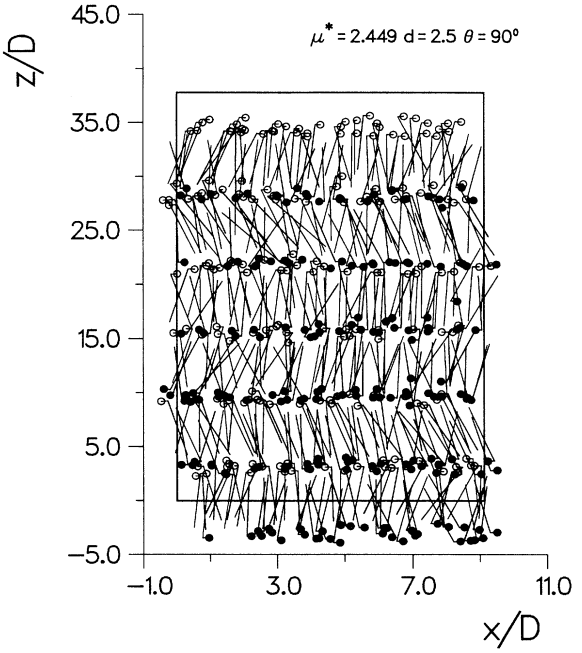

FIG. 9. Snapshot of a configuration of 384 spherocylinders with transverse dipole moment $\mu^*=2.449$ located at distance $d=2.5$ from the center of the molecule in the smectic-A phase ($p^*=3.8$) (projection on the xz plane of the periodic box; the molecules are represented by thin lines of length $5D$). Circles represent the dipole-moment positions. Open circles, molecular axis (oriented from the center of the molecule to the dipole moment) pointing in the positive z direction. Solid circles, molecular axis pointing in the negative z direction.

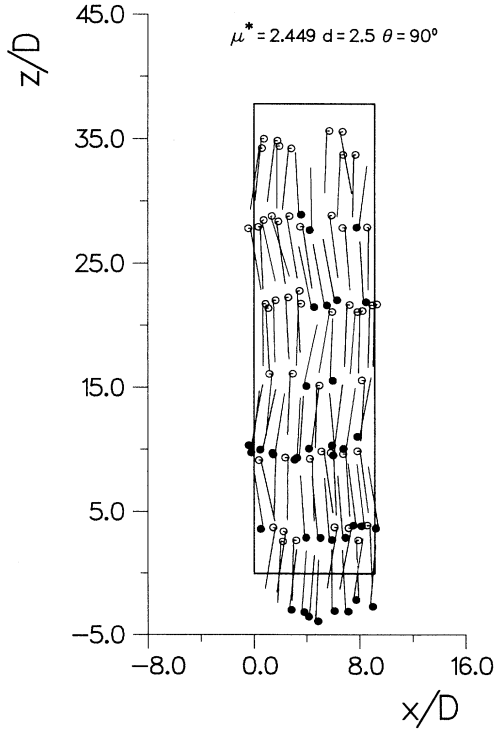

FIG. 10. Same as Fig. 9, but for molecules in a slice of width $\Delta y \simeq 2D$ in the y direction. The scales in the x and z directions are identical.

been confirmed more quantitatively by showing that the average total dipole moment of the molecules within each layer was vanishing. Also, there is considerable interpenetration of the dipolar heads which allows the system to lower its energy. For instance, at $\mu^*=2.449$, $p^*=3.8$, the internal energy $\beta U/N=-2.04$. In contrast, in a system in which the centers of mass are constrained to lie in ideal smectic planes but the interplane distance allowed to fluctuate (as is obviously possible in a NpT calculation), the energy per particle is $+5.3$ at the same pressure $p^*=3.8$.

Figure 11 shows the projection on the xy plane of the dipole moments in a typical interface region between two layers. Despite the strength of the dipole moments, there is no obvious correlation between the positions of dipolar heads pointing "up" (dashed line) and "down" (solid line). We stress that the low value of the energy is due to fluctuations of the positions of the polar heads rather than to formation of some permanent ordering of the heads in the interface region.

As already stated above, the location of the dipolar heads is much stronger in the case of a transverse dipole moment resulting in a weaker interpenetration of the smectic layers as compared to the longitudinal case. This is also apparent from the snapshots given in Figs. 9 and 10. The dipolar arrangement in the region separating two layers is shown in more detail in Fig. 12. Although some care should be taken in inferring general behavior from instantaneous snapshots, there seems to be a trend to dipolar ordering in which domains are formed with the dipole moments aligning in a parallel way. Such an arrangement is energetically favorable if the dipole moments are nearly in plane. There is no indication of bilayer formation such that the polar heads of two adjacent layers would preferentially be in contact. In each layer there is, on the average, an equal number of polar heads pointing "up" and "down." In our calculations we observe a global polarization of the system parallel to the smectic plane. However, we believe that the lengths of the present Monte Carlo runs are too short to decide unambiguously whether this polarization is an artifact due to insufficient sampling of configuration space or whether there is a tendency of the system to have ferroelectric behavior as suggested in recent literature [20,22]. We intend to investigate this possibility by performing longer runs including the nematic phase.

Additional computations were performed for a dipole moment making an angle $\theta=60°$ with the molecular long axis. For this case the structural properties of the smectic phase were found to be quite similar to those with $\theta=90°$, and thus there is no need to give further details. However, we would like to stress that for all values of θ, the preferential alignment direction of the molecules was

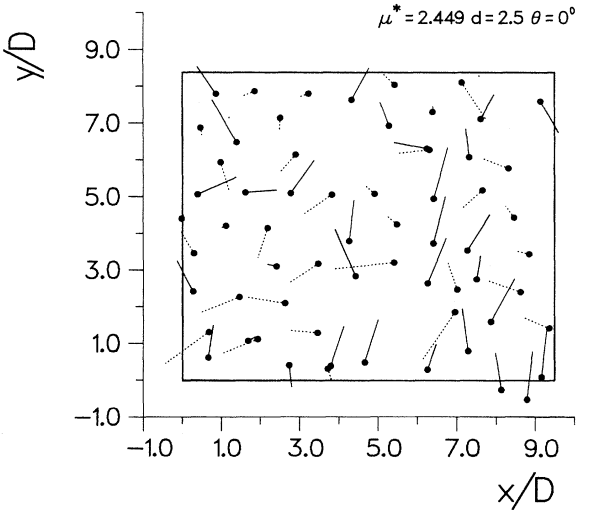

FIG. 11. Projection on the xy plane (parallel to the smectic plane) of the molecules inside the contact region of two adjacent layers in the smectic-A phase ($p^*=3.8$). Snapshot of dipolar spherocylinders with longitudinal dipole moment $\mu^*=2.449$ located at a distance $d=2.5$ from the center. The molecules are represented by thin lines of length $5D$ and the location of the dipole moment is indicated by the solid circle. Solid (dotted) lines represent dipole moments pointing in the negative (positive) z direction.

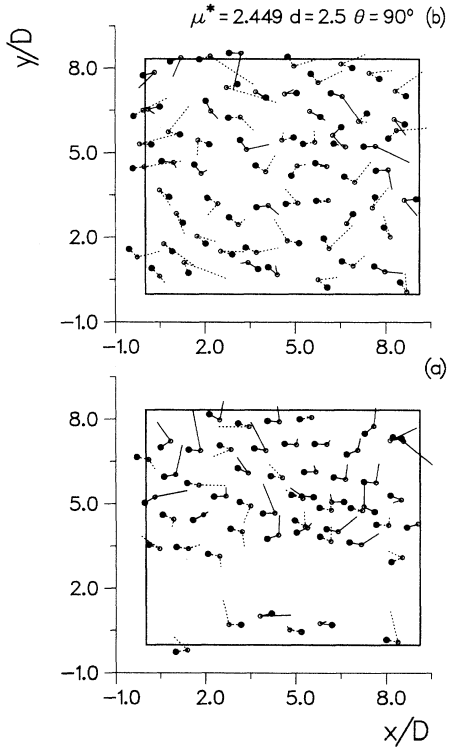

FIG. 12. Projection on the xy plane (parallel to the smectic plane) of the molecules inside the contact region of two adjacent layers in the smectic-A phase ($p^*=3.8$). Snapshot for dipolar spherocylinders with transverse dipole moment $\mu^*=2.449$ located at a distance $d=2.5$ from the center. The molecules are represented by thin lines of length $5D$ and the dipoles by thin lines of arbitrary length originating at an open circle and terminating at a solid circle. Solid (dotted) lines represent molecules with symmetry axes (oriented from the center of the molecule to the dipole moment) pointing in the negative (positive) z direction. (a) The contact region corresponds to the region near $z/D\sim 15$ in Fig. 9; (b) the contact region corresponds to the region near $z/D\sim 27$ in Fig. 9.

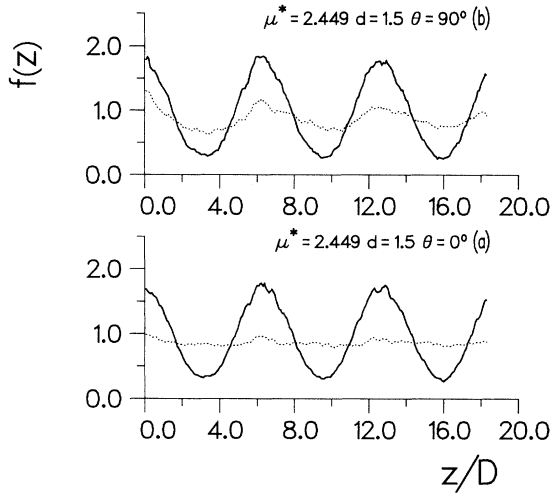

FIG. 13. Density modulation [Eq. (5)] of the smectic-A phase of dipolar spherocylinders with $\mu^*=2.449$ and $d=1.5$ ($p^*=3.8$). Solid line, center-of-mass density; dotted line, density of dipole-moment positions. (a) $\theta=0°$; (b) $\theta=90°$.

always perpendicular to the smectic planes. There is no tendency for tilt of the director with respect to the smectic layer normal.

2. $d=1.5$ and $d=0$

We further explored the possibility for a strong longitudinal dipole moment located somewhat deeper inside the molecular core to induce a smectic phase with overlapping molecular cores and antiparallel ordering of the dipole moments. Towards this end, we performed a Monte Carlo simulation at $p^*=3.8$, $\mu^*=2.449$, and the dipole moment located half-way between the molecular center and end ($d=1.5$). The density correlation functions (Fig. 13) and snapshots (Figs. 14 and 15) reveal, however, that the structure of the smectic phase is not very different from the one obtained with a dipole moment located near one molecular end. Because of the rather large positional and orientational fluctuations of the molecules around their average values, the average distribution of dipolar centers along the z directions is now nearly uniform (cf. Fig. 13). Finally, moving the dipole moment to the center of the spherocylinder ($d=0$) still results in quite similar smectic phase behavior. The center-of-mass density correlation function for $\mu^*=2.449$, $\theta=60°$ is shown in Fig. 16. It is indistinguishable, within statistical error, from the corresponding function obtained for a system of nonpolar molecules [cf. Fig. 1(c) of Ref. [21]].

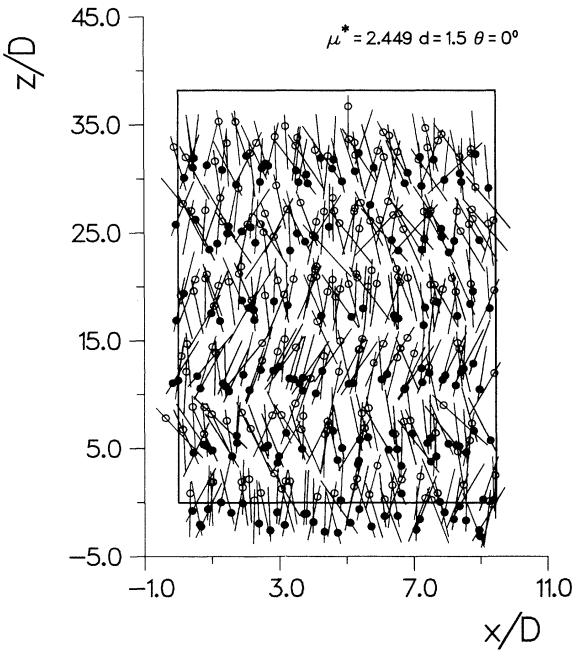

FIG. 14. Snapshot of a configuration of 384 spherocylinders with longitudinal dipole moment $\mu^*=2.449$ located at distance $d=1.5$ from the center of the molecule in the smectic-A phase ($p^*=3.8$) (projection on the xz plane of the periodic box; the molecules are represented by thin lines of length $5D$). Circles represent the dipole-moment positions. Open circles, dipole moments pointing in the positive z direction; solid circles, dipoles pointing in the negative z direction.

IV. CONCLUSION

In this paper we have addressed the question of mesophase structure in a simple liquid-crystal model formed by dipolar spherocylinders using Monte Carlo simula-

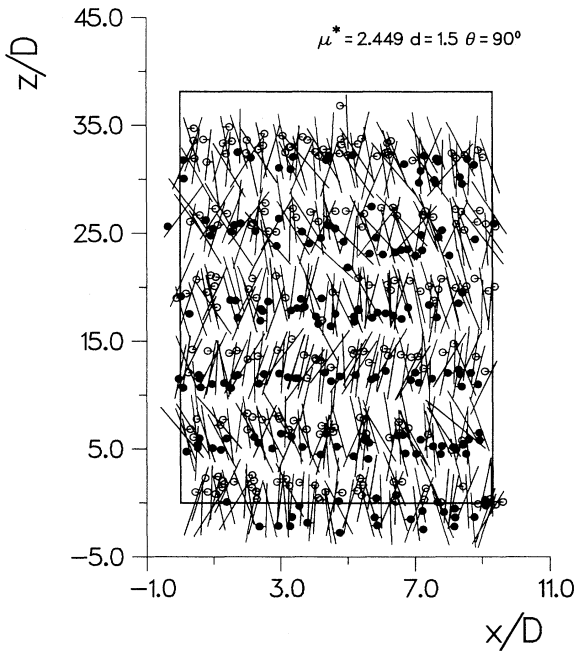

FIG. 15. Snapshot of a configuration of 384 spherocylinders with transverse dipole moment $\mu^*=2.449$ located at distance $d=1.5$ from the center of the molecule in the smectic-A phase ($p^*=3.8$) (projection on the xz plane of the periodic box; the molecules are represented by thin lines of length $5D$). Circles represent the dipole-moment positions. Open circles, molecular axis (oriented from the center of the molecule to the dipole moment) pointing in the positive z direction; solid circles, molecular axis pointing in the negative z direction.

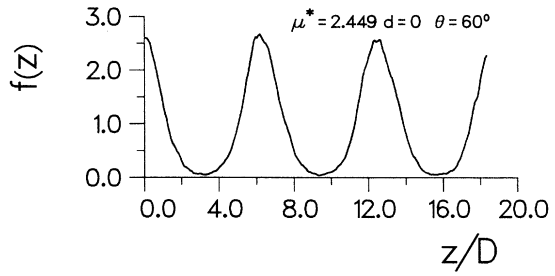

FIG. 16. Center-of-mass density modulation of the smectic-A phase of dipolar spherocylinders with central dipole moment making an angle $\theta=60°$ with the molecular symmetry axis. The pressure is $p^*=3.8$.

tions. Present-day theoretical approaches (at a microscopic level) are much too crude to provide more than a qualitative answer [23–27] or are restricted to the isotropic phase [28]. Special emphasis has been given to the smectic phase. For effective dipole moments representative of those encountered in strong dipolar cyano or nitro groups, a monolayer smectic Sm-A_1 structure with layer distance approximately equal to one molecular length is found and this for all locations of the dipole moment varying from the center of the molecule to one of its ends and for all direction varying from parallel to perpendicular to the molecular symmetry axis. The layers are unpolarized and no trend for antiparallel association of dipole moments in adjacent layers is observed for longitudinal dipole moments. In the case of a transverse dipole moment, there is some evidence for ferroelectric behavior, although we hasten to stress that it has to be verified that it is not an artifact of insufficient sampling of configuration space in the Monte Carlo simulations.

The monolayer smectic phase is not the one most commonly found in polar compounds, which is rather of a partial bilayer type with appreciable overlap of the molecular cores [11]. The reason for the occurrence of a monolayer phase lies probably in the very symmetrical nature of the hard-core part of our model. In this model the shape of the molecule is represented by a rigid cylinder which contains the volume of rotation obtained by rotating the molecule about its long axis. Such an oversimplified model is clearly all the more inappropriate the more bent or distorted the molecular shape is, as it severely restricts nearest-neighbor packing arrangements that could be obtained by interpenetration of the molecular cores. The situation is certainly even much more subtle. Sm-A_1 phases are not observed in short polar molecules, as, for instance, the commonly studied cyanobiphenyls (they give Sm-A_d phases [11,29]), but are observed in the somewhat longer polar compounds of the structural form

$$C_nH_{2n+1}O—\phi—COO-\phi-Y-\phi-\mathcal{R}$$

where ϕ denotes a phenyl group, $\mathcal{R}$ a strongly polar cyano (CN) or nitro (NO_2) head group. The linkage Y may be a —C≡C—, —CH=CH—, or —OOC— group [11,30,31]. A maximum stability of the Sm-A_1 phase is obtained with 4–5 methylene groups, and it is destabilized in favor of a reentrant nematic phase when $n\sim 8-9$, indicating the definite role of the tail chain [11]. In addition, there is experimental evidence for the importance on phase stability of the orientation of the ester linkage (and thus of the dipole-moment orientation) at position Y. For instance, a low-temperature monolayer phase is observed when $Y=$OOC (dipole moment opposite to that of the terminal group) but not for $Y=$COO (dipole moment in the same direction as that of the terminal group) [31]. The effects of the various factors mentioned above on smectic phase stability clearly need further theoretical investigation.

In the present simulations, only the mechanical stability of the mesophases has been established, a precise location of the different phases based on free-energy calculations (thermodynamic stability) being beyond the scope of this study. Common belief is that dipole-dipole forces do not play a significant role in determining phase stability [32]. This question will be taken up in a future publication, including the study of the nematic phase.

ACKNOWLEDGMENTS

G.J.Z. acknowledges financial support from Fundación Antorchas (Argentina); Carrera del Investigador Científico, Commisón de Investigaciones Científicas de la Provincia de Buenos Aires; and the ICSC World Laboratory. The Laboratoire de Physique Théorique et Hautes Energies is "laboratoire associé au Centre National de la Recherche Scientifique."

*Permanent address: IFLYSIB, Facultad de Ciencias Exactas, UNLP–C.C. 565, 1900 La Plata, Argentina.

[1] See, e.g., G. Vertogen and W. H. de Jeu, *Thermotropic Liquid Crystals, Fundamentals* (Springer, Heidelberg, 1988).
[2] M. P. Allen, D. Frenkel, and J. Talbot, J. Comput. Phys. Rep. **9**, 301 (1989).
[3] D. Frenkel and B. M. Mulder, Mol. Phys. **55**, 1171 (1985).
[4] D. Frenkel, J. Phys. Chem. **92**, 3280 (1988).
[5] J. A. C. Veerman and D. Frenkel, Phys. Rev. A **41**, 3237 (1990).
[6] M. P. Allen, Liq. Cryst. **8**, 499 (1990).
[7] R. Eppenga and D. Frenkel, Mol. Phys. **52**, 1303 (1984).
[8] D. Frenkel, Liq. Cryst. **5**, 929 (1989).
[9] J. A. C. Veerman and D. Frenkel, Phys. Rev. A **45**, 5632 (1992).
[10] G. J. Zarragoicoechea, D. Levesque, and J. J. Weis (unpublished).
[11] F. Hardouin, A. M. Levelut, M. F. Achard, and G. Sigaud, J. Chim. Phys. **80**, 53 (1983).
[12] G. Sigaud, F. Hardouin, M. F. Achard, and A. M. Levelut, J. Phys. (Paris) **42**, 107 (1981); K. K. Chan, P. S.

Pershan, L. B. Sorensen, and F. Hardouin, Phys. Rev. A **34**, 1420 (1986); F. Hardouin, Physica A **140**, 359 (1986).
[13] P. E. Cladis, Phys. Rev. Lett. **35**, 48 (1975); Mol. Cryst. Liq. Cryst. **165**, 85 (1988).
[14] J. Prost and P. Barois, J. Chim. Phys. **80**, 65 (1983); J. Prost. Adv. Phys. **33**, 1 (1984).
[15] S. W. de Leeuw, J. W. Perram, and E. R. Smith, Proc. R. Soc. London Ser. A **373**, 27 (1980).
[16] M. P. Allen and D. J. Tildesley, *Computer Simulation of Liquids* (Clarendon, Oxford, 1987).
[17] J. W. Perram and M. S. Wertheim, J. Comput. Phys. **58**, 409 (1985).
[18] G. J. Zarragoicoechea, D. Levesque, and J. J. Weis, Mol. Phys. **74**, 629 (1991).
[19] G. J. Zarragoicoechea, D. Levesque, and J. J. Weis, Mol. Phys. **75**, 989 (1992).
[20] D. A. Dunmur and K. Toriyama, Mol. Cryst. Liq. Cryst. **198**, 201 (1991).
[21] J. J. Weis, D. Levesque, and G. J. Zarragoicoechea, Phys. Rev. Lett. **69**, 913 (1992).
[22] P. Palffy-Muhoray, M. A. Lee, and R. G. Petschek, Phys. Rev. Lett. **60**, 2303 (1988).
[23] R. B. Meyer and T. C. Lubensky, Phys. Rev. A **14**, 2307 (1976).
[24] F. Dowell, Phys. Rev. A **31**, 3214 (1985).
[25] J. O. Indekeu and A. N. Berker, Phys. Rev. A **33**, 1158 (1986).
[26] R. R. Netz and A. N. Berker, Phys. Rev. Lett. **68**, 333 (1992).
[27] M. Baus and J. L. Colot, Phys. Rev. A **40**, 5444 (1989).
[28] A. Perera and G. N. Patey, J. Chem. Phys. **91**, 3045 (1989).
[29] A. J. Leadbetter, J. C. Frost, J. P. Gaughan, G. W. Gray, and A. Mosley, J. Phys. (Paris) **40**, 375 (1979); A. J. Leadbetter and A. I. Mehta, Mol. Cryst. Liq. Cryst. Lett. **72**, 51 (1989).
[30] N. H. Tinh, J. Chim. Phys. **80**, 83 (1983).
[31] Y. Sakurai, S. Takenaka, H. Sugiura, S. Kusabayashi, Y. Nishihata, H. Terauchi, and T. Takagi, Mol. Cryst. Liq. Cryst. **201**, 95 (1991).
[32] K. Toriyama and D. A Dunmur, Mol. Phys. **56**, 479 (1985).